WARSAW UNIVERSITY OF TECHNOLOGY Index 351733
FACULTY OF CIVIL ENGINEERING
COMMITTEE FOR CIVIL AND WATER ENGINEERING
POLISH ACADEMY OF SCIENCES ISSN 1230-2945

DOI: 10.24425/ace.2024.149856

ARCHIVES OF CIVIL ENGINEERING

Vol. LXX ISSUE 2 2024

pp. 149 –162

Research paper

Relationship between deflection basin parameters and backcalculated pavement layer moduli

Mateusz Kałuża[1], Mirosław Kotasiński[2]

Abstract: In the case analysed, a glass fibre mesh was applied under the asphalt layer during a rehabilitation treatment. Because only one lane was reinforced, the test section can be used to observe the influence of glass fibre mesh on the relationship between the selected deflection basin parameters (RoC, BLI, MLI, and LLI) and back-calculated pavement layer moduli. The FWD measures were used to determine the bowl of deflection indicators and to back-calculate the layer's moduli. The values of DBP-s allowed confirmation of the technical condition of pavement construction. The first measures were carried out in 2019 and repeated in 2021; the results were then compared and analysed. Influence was observed on the relationship between the deflection basin and moduli, especially for the base course and subgrade. The reinforced lane showed a better coefficient of determination between DBPs and moduli in 2019, but in 2021 relationships were observed only for LLI and subgrade moduli. The unreinforced lane, however, showed the mentioned relationships in both 2019 and 2021. Because of a relatively small number of measurement points, the presented analyses and observations should be considered as preliminary. Presented results and relationships are another step into developing an alternative approach to determining the initial pavement moduli i.e. to use as a seed moduli.

Keywords: deflection basin parameters, FWD, geogrid, pavement reinforcement, terrain subsidence

[1]MSc., Eng., Silesian University of Technology, Faculty of Civil Engineering, Akademicka 5, 44-100 Gliwice, Poland, e-mail: mateusz.kaluza@polsl.pl, ORCID: 0000-0002-9761-9066

[2] PhD., Eng., Silesian University of Technology, Faculty of Civil Engineering, Akademicka 5, 44-100 Gliwice, Poland, e-mail: miroslaw.kotasinski@polsl.pl, ORCID: 0000-0002-5588-0741

1. Introduction

The analysed road section was rehabilitated in 2008 by milling the existing asphalt layers and applying new ones – 3–6 cm of levelling course, 6 cm of binder course, and 4 cm of the surface course. The right lane was reinforced with a glass fibre mesh (break strength 50/50 kN/m with break elongation 3%) applied to the existing construction under the base course. The left lane was left without reinforcement, as shown in Fig. 1. The existing structure consists of 20 cm of an aggregate base layer and 20 cm of crushed stone subgrade. It lies in the mining area of the 1st category, and the measured total subsidence from 2008 to 2019 was around 10 cm.

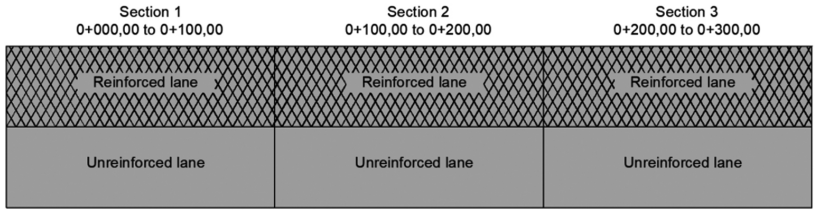

Fig. 1. Analysed road section scheme

Ten years after rehabilitation treatment, the authors decided to investigate the effectiveness of the applied solutions, keeping in mind the influence of continuous mining subsidence. The main objective of this paper is to identify the impact of applied reinforcement on the relationship between the chosen deflection basin parameters and the backcalculated pavement moduli. The use of the geosynthetic layer as a subgrade reinforcement under mining influences in flexible pavement construction has been widely described [1–5]. The application directly on top of the old asphalt layer under the overlay allows delay or prevents crack propagation between layers [6–11]. The increase in pavement fatigue resistance was proven. The application below the subbase reduces the influence of horizontal unloosing strain and is the most effective solution [1, 15] Thus, it improves the resistance of the entire pavement construction to the loss of the equilibrium state from mining subsidence [1–3]. With the proper type of geosynthetic, the stiffness and bearing capacity of the asphalt layers is increased; interlocking with asphalt concrete contributes to the restraining effect [7, 8].

The correlations between selected deflection basin parameters and pavement moduli were previously studied to determine the limit values of the deflection basin parameters for the equivalent required module of pavement construction [16]. Recent research has shown that the relationships between some DBPs and the moduli of the pavement layers may be useful to determine seed moduli used for the backcalculation [17, 18]. There is still a large gap to be addressed in the matter of beforementioned relationships.

2. Materials and research methods

To investigate the subgrade and the existing pavement layers, three drillings of 4.0 m deep were performed. Pavement construction consists of the following layers:

1. asphalt concrete – 12–18 cm,
2. crushed stone aggregate – 35–45 cm,
3. embankment (sand, crushed stone) – 60 cm.

The subgrade below the embankment differs from fine sands with clay sand in the medium dense state through stiff clay silt to silt sands with layers of fine silt in the medium dense state. For the backcalculation, the subgrade was unified. Subgrade moduli E_{sub} range from 43 to 70 MPa. The deflections were measured with a falling weight deflectometer (FWD) under a dynamic load of 50 kN. Geophones ($D_0 - D_9$) were set in the distances shown in Fig. 2. Measurements were taken in the mark of the right wheel every 25 m in each lane. The tests were carried out in August 2019 and September 2021.

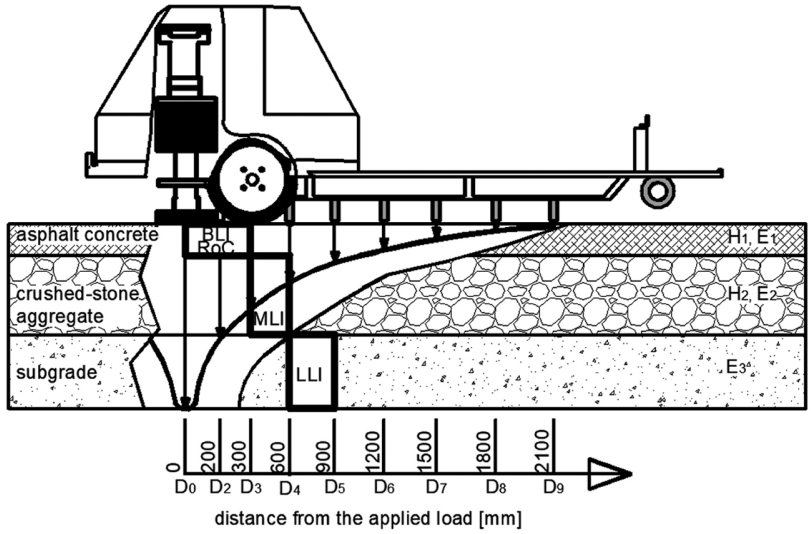

Fig. 2. Falling weight deflectometer with a bowl of deflection and curvature indexes shown on a corresponding layer of pavement construction

The data were used to determine the parameters of the deflection bowl (DBP) and to backcalculate the moduli of the pavement layers. The results were then compared to analyse the influence of applied reinforcement on the relationship between moduli and DBPs. In this article, the deflection basin parameters such as the base layer index, the middle layer index, the lower layer index, and the radius of curvature were chosen for further analysis because they accurately correlate with the strains observed at the bottom of the asphalt layer [12–14]. These strains are crucial for the asphalt fatigue criterion to properly determine the remaining structural and functional life of the pavement. The following DBP-s were used in the analysis:

– BLI (Base Layer Index, also called Surface Curvature Index SCI) characterises the condition of the pavement layers:

$$\text{BLI} = D_0 - D_{300} \tag{2.1}$$

where: D_0 – maximum deflection [μm], D_{300} – deflection measured with the load cell at a distance of 300 mm [μm].

– MLI (Middle Layer Index, also called Base Damage Index) characterises the condition of the base layer:

$$\text{MLI} = D_{300} - D_{600} \tag{2.2}$$

where: D_{600} – deflection measured with the load cell at a distance of 600 mm [μm].

– LLI (Lower Layer Index, also called Base Curvature Index) characterises the condition of the subgrade:

$$\text{LLI} = D_{600} - D_{900} \tag{2.3}$$

where: D_{900} – deflection measured with a load cell at a distance of 900 mm [μm].

– RoC (Radius of Curvature) characterises the condition of the pavement layer and base layer:

$$\text{RoC} = \frac{L^2}{2D_0\left(1 - \frac{D_{200}}{D_0}\right)} \tag{2.4}$$

where: $L = 200$ mm for the FWD, D_{200} – deflection measured with a load cell at a distance of 200 mm [μm],

The next step included the backcalculation of the layer moduli carried out with the ELMOD software. The basin fit methodology was used to estimate the moduli. The theoretical deflection bowl for a particular pavement construction is calculated and compared to the measured deflections to determine the error. Then, the moduli of the layers are decreased or increased, and the procedure is repeated until the minimum values in error between calculated and measured deflections bowls are found. It is important to remember that different combinations of layer stiffness may produce the same bowl of deflection, and thus give improper values within the small range of error. This occurs more often in 4 and 5 layer pavement models and because of that similar layers were combined to create a 3 layer model. The mm moduli for asphalt concrete, subbase, and subgrade were calculated. The value of the deflection of the bowl is described with the following equation:

$$U_i = f(h, E, \nu) \tag{2.5}$$

where: U_i – deflection value at the i-point [μm], f – functional dependence of component factors, h – thickness of each pavement layer [mm], E – moduli of the pavement layer [MPa], ν – Poisson's ratio [–].

The bowl of deflection shape is determined by the thickness of the analysed layer, the value of the moduli of the layer, and the value of the Poisson ratio. Subgrade moduli affect the deflection bowl noticeably, moving the whole deflection bowl up when the moduli values rise and moving the bowl down when the moduli value lowers. Measured deflections were standardized to a load of 50 kN and a temperature of 20°C. The Poisson ratio value used for backcalculation was $\nu = 0.30$ for every layer. The asphalt layers moduli E_1 were adjusted to the temperature of 20°C, as shown in Table 1. For backcalculation, two pavement models with different thicknesses of the AC layers were used:

– section 1 – km 0+000 to 0+100, 12 cm of asphalt concrete, 40 cm of crushed stone aggregate, subgrade,
– section 2 – km 0+100 to 0+200, 17 cm of asphalt concrete, 40 cm of crushed stone aggregate, subgrade,
– section 3 – km 0+200 to 0+300, 12 cm of asphalt concrete, 40 cm of crushed stone aggregate, subgrade.

3. Results and discussion

At the beginning, the values of the deflection basin parameters, which describe the upper layers of construction, were compared with the backcalculated AC moduli, separately for the reinforced and unreinforced lanes. The results for the year 2019 are shown in Table 1. The power function was used to determine the relationship between parameters. As for the DBP-s describing the technical condition of the layer, higher value of the radius of curvature indicate a better technical condition of the layer, opposite to the rest of the DBP-s, where lower values indicate the better condition. The logical conclusion is that with higher value of AC moduli, the RoC value should increase and the BLI value will do the opposite. Due to a relatively small number of measurement points, the following analysis focusses on determining whether the relationship occurs as a preliminary investigation. Figures 3 and 4 show the results representing a good relationship between DBP-s and the moduli ($R^2 = 0.58 \div 0.80$); the reinforced lane produces a better correlation for both, RoC and BLI indicators.

Table 1. Backcalculated layer moduli and deflection basin parameters for the measures taken in 2019

Chainage	BLI [μm]	MLI [μm]	LLI [μm]	RoC [μm]	E_1 [MPa]	$E_{1,\mathrm{tr}}$ [MPa]	E_2 [MPa]	E_{sub} [MPa]
Unreinforced lane								
0+000	330	161	79	90	813	1393	203	64
0+025	227	144	70	141	1582	2710	196	81
0+050	164	90	37	186	1967	3370	300	90
0+075	207	124	54	153	1722	2950	222	111
0+100	200	131	71	153	1638	2806	283	56
0+125	187	145	85	145	1152	1974	285	35
0+150	255	181	95	124	954	1634	148	45
0+175	210	160	89	149	1186	2032	164	50
0+200	399	259	131	75	555	951	109	35
0+225	189	157	58	158	2001	3428	215	66
0+250	232	179	92	133	1719	2945	179	52
0+275	242	150	81	131	1470	2518	205	65
0+300	232	138	66	142	1480	2536	263	52

Continued on the next page

Continued from the previous page

Chainage	BLI [μm]	MLI [μm]	LLI [μm]	RoC [μm]	E_1 [MPa]	$E_{1,tr}$ [MPa]	E_2 [MPa]	E_{sub} [MPa]
Reinforced lane								
0+000	302	219	115	101	1347	2308	125	63
0+020	257	190	94	124	1619	2774	158	54
0+045	202	115	43	154	1845	3161	188	55
0+070	263	156	77	112	1131	1938	235	56
0+095	153	120	70	225	2925	1700	257	60
0+120	254	132	55	127	885	1516	151	44
0+145	260	218	119	125	1044	1789	131	28
0+170	155	146	89	217	1885	3229	172	39
0+195	347	217	125	93	696	1192	116	39
0+220	318	211	104	102	1226	2100	137	51
0+245	243	171	77	137	1729	2962	150	81
0+270	251	171	73	142	1772	3036	131	100
0+295	281	175	68	114	1339	2294	154	85

*E_1 – asphalt layers module,
$E_{1,tr}$ – asphalt layers module adjusted to the temperature of 20°C,
E_2 – crushed stone aggregate module, E_{sub} – subgrade module.

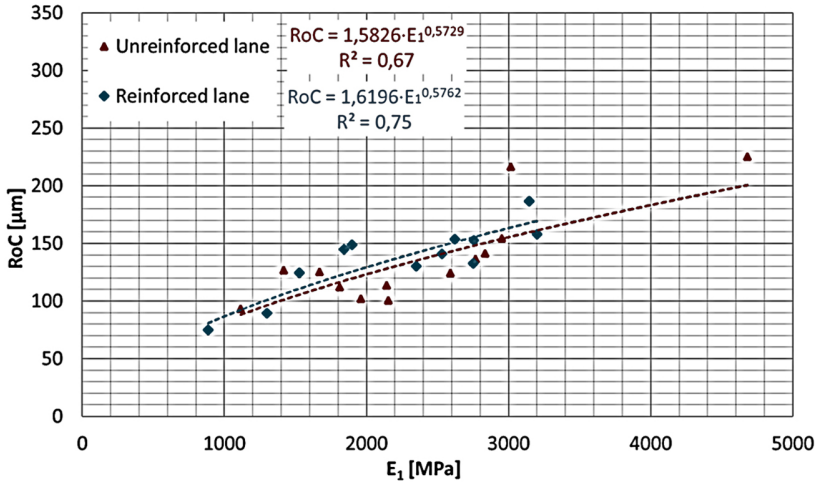

Fig. 3. A comparison of the radius of curvature (RoC) with asphalt concrete moduli (E_1) for the measures taken in 2019

The values of R^2 obtained in this study are similar or better to those obtained by Talvik and Aavik [16] for the correlations between upper layers indicators and equivalent pavement modulus. The radius of curvature relationship with asphalt module differs lower than the

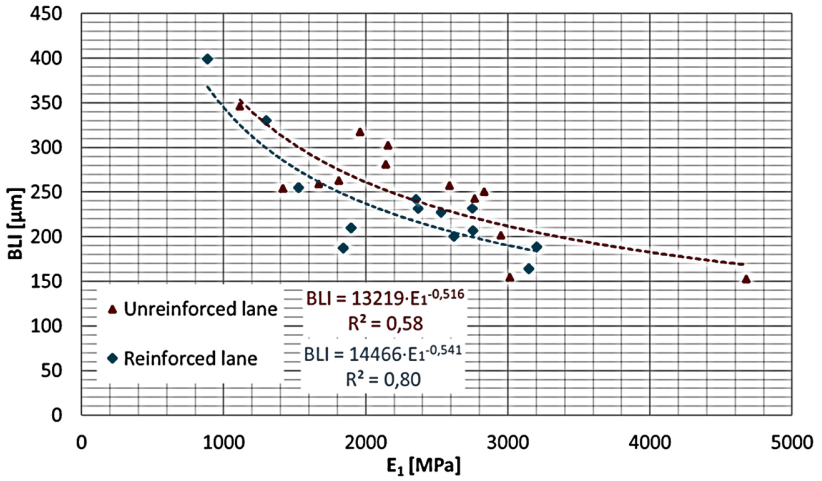

Fig. 4. A comparison of the base layer index (BLI) with the asphalt concrete moduli (E_1) for the measures taken in 2019

relationship with base layer index. When analysing the layers below the asphalt concrete, it is worth noting that for the middle layer index (MLI) and the lower layer index (LLI), lower values indicate a better technical condition. For the relation MLI–E_2, shown in Fig. 5, the values of R^2 are around 0.61 for the unreinforced lane and 0.83 for the reinforced lane, indicating a very good relationship similar to the relationship observed previously for RoC–E_1 and BLI–E_1. Again, a stronger correlation is observed in the reinforced lane. This may suggest the influence of the applied reinforcement between the AC layers and the base layers. For the relation LLI–E_{sub}, shown in Fig. 6, the values of R^2 are around 0.71 for the unreinforced lane and 0.75 for the reinforced lane, indicating the existence of the relationship independently of the applied reinforcement.

The second FWD measurement performed in 2021 was used to validate the previous analysis. The results are presented in Table 2. For RoC-E1, the relationship is present in the unreinforced lane ($R^2 = 0.77$) but is very weak in the reinforced lane ($R^2 = 0.31$). This trend continues for the BLI–E_1 relationship, where is it similar in 2021 as was in 2019 in the unreinforced lane, but becomes non-existant for the reinforced lane ($R^2 = 0.07$). Again, difference between lanes is lower for RoC–E_1, but values for the reinforced lane are very low. For the MLI–E_2 relation shown in Fig. 9, the values of R^2 are around 0.71 for the unreinforced lane and 0.07 for the reinforced lane. For the LLI-E_{sub}, as shown in Fig. 10, the values of R^2 are around 0.61 for the unreinforced lane and 0.88 for the reinforced lane. The results show that the analysed relationships are weaker for the reinforced lane in 2021 than they were in 2019, except for LLI–E_{sub} which seems unaffected directly by the applied reinforcement. It is a similar situation to those observed in previous researches, where strong relationships occurred between subgrade moduli and lower layer index LLI ($R^2 > 0.80$) in the latest researches by Rocha et al. [17]. The opposite conclusions were formulated by Talvik and Aavik, who pointed that good correlation was observed between

Table 2. Backcalculated layers moduli and deflection basin parameters for the measures taken in 2021

Chainage	BLI [μm]	MLI [μm]	LLI [μm]	RoC [μm]	E_1 [MPa]	$E_{1,\mathrm{tr}}$ [MPa]	E_2 [MPa]	E_{sub} [MPa]
Unreinforced lane								
0+000	401	242	113	84	1086	1158	122	58
0+025	261	183	83	116	1528	1629	200	64
0+050	247	207	98	149	2339	2493	117	77
0+076	167	152	72	211	3703	2507	166	93
0+100	192	140	72	167	2364	2520	237	80
0+125	229	146	66	139	1124	1198	187	83
0+150	192	173	100	173	1609	1715	182	35
0+175	195	181	113	168	1608	1714	165	33
0+200	218	202	120	161	1515	1615	117	41
0+225	266	230	140	128	2031	2165	147	34
0+251	120	115	71	284	4807	2676	221	62
0+275	166	138	84	203	2990	3187	215	53
0+300	212	162	81	140	1813	1933	249	58
Reinforced lane								
0+010	168	159	91	215	6983	3100	104	86
0+034	255	226	106	139	2967	3163	117	57
0+060	223	148	62	148	2350	2505	194	59
0+085	270	184	94	135	2126	2266	171	60
0+110	179	164	99	195	1877	2001	132	59
0+135	218	136	66	139	1132	1207	213	86
0+159	202	178	106	166	1534	1635	161	39
0+185	227	187	95	151	1359	1449	130	57
0+215	310	278	152	111	1844	1966	130	26
0+239	257	211	118	133	2033	2167	158	42
0+265	223	183	92	153	2485	2649	143	78
0+290	242	206	101	144	2282	2433	160	58

*E_1 – asphalt layers module,
$E_{1,tr}$ – asphalt layers module adjusted to the temperature of 20°C,
E_2 – crushed stone aggregate module, E_{sub} – subgrade module.

asphalt module and DBPs describing the upper layers of pavement. The results comparision between 2019 and 2021 indicates that technical condition of the road affects obtained correlations. Additionally, in this study the influence of thickness of pavement layers on the analysed relationships was not investigated. This may led to the situation where some of the deflection basin parameters are influenced by the moduli of different layers which they are not suppose to describe. The best example would be the Base Layer Index (BLI) calculated for the asphalt layer thinner than the radius of the FWD plate. This needs further investigation on how the thicknesses impact the results.

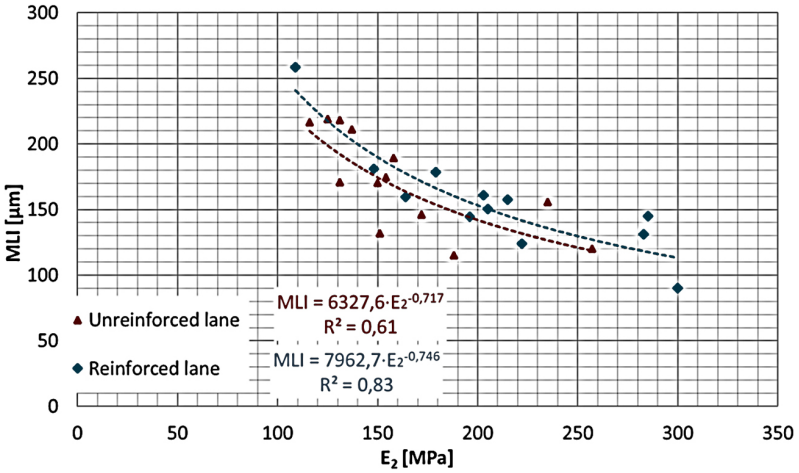

Fig. 5. A comparison of the middle layer index (MLI) with the base layer moduli (E_2) for the measures taken in 2019

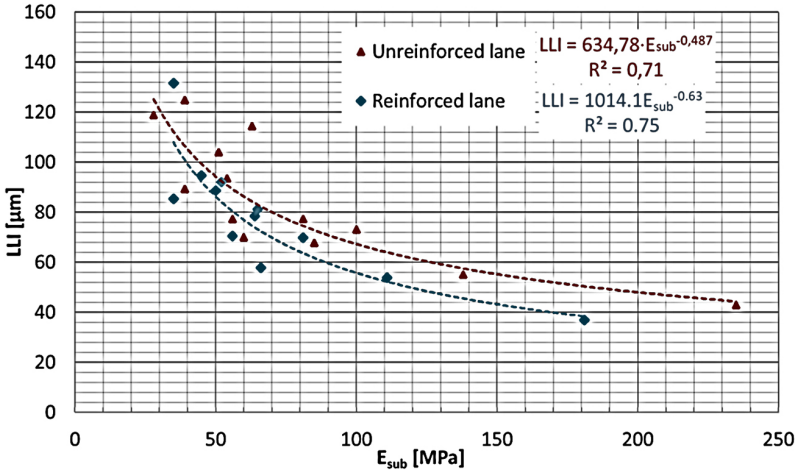

Fig. 6. A comparison of the lower layer index (LLI) with the subgrade moduli (E_{sub}) for the measures taken in 2019

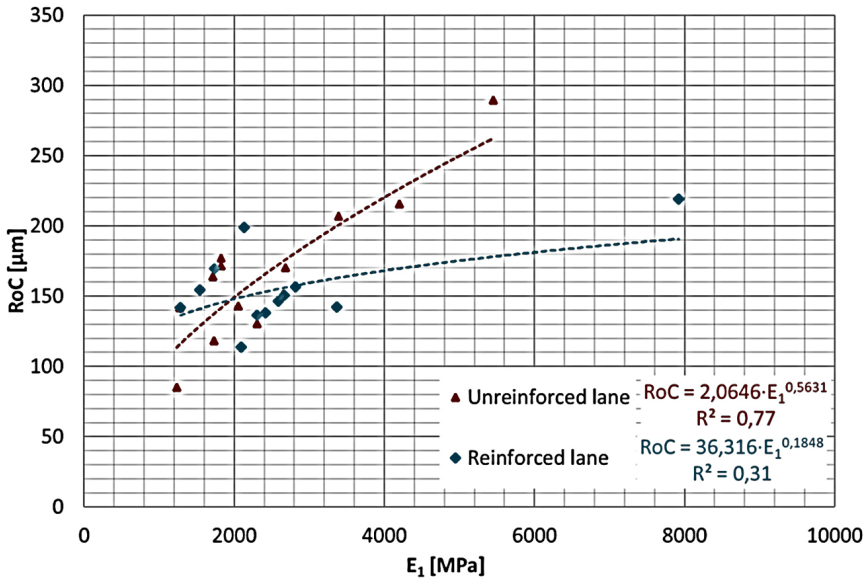

Fig. 7. A comparison of the radius of curvature (RoC) with asphalt concrete moduli (E_1) for the measures taken in 2021

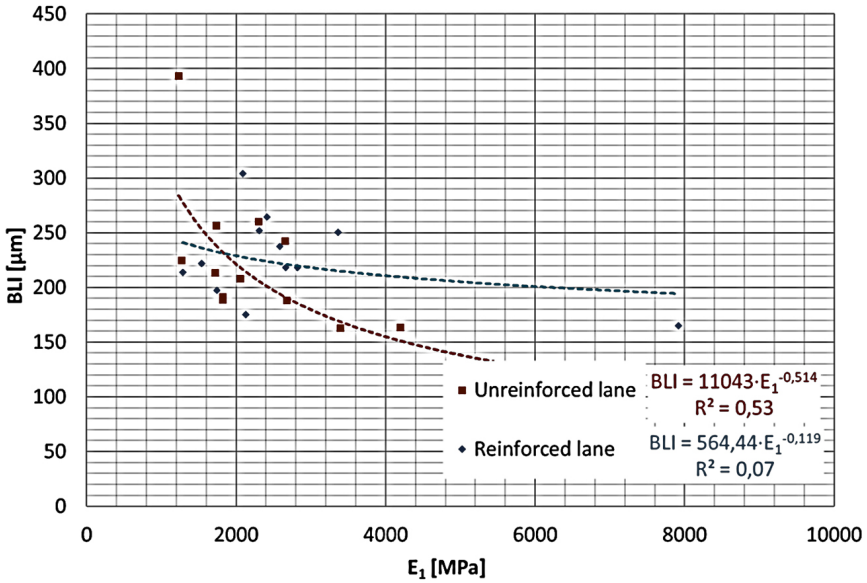

Fig. 8. A comparison of the base layer index (BLI) with the asphalt concrete moduli (E_1) for the measures taken in 2021

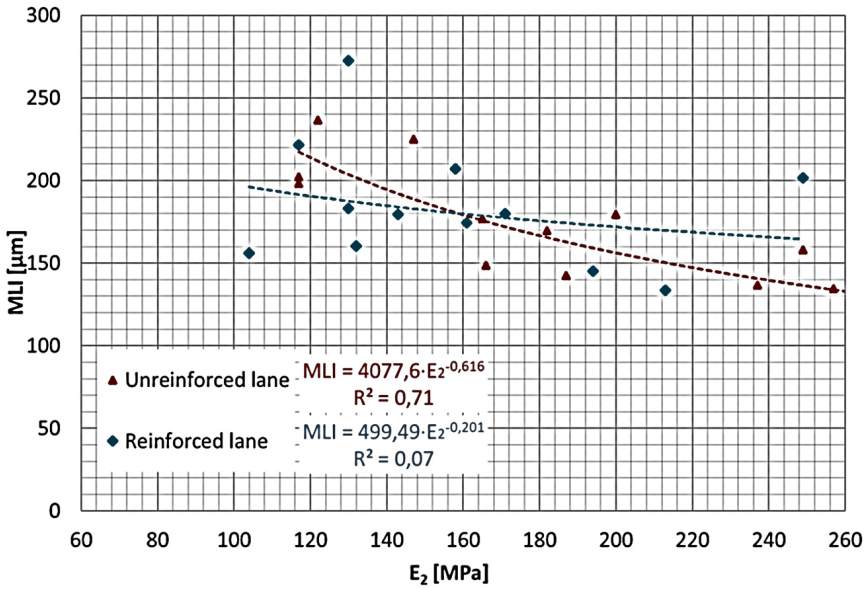

Fig. 9. A comparison of the middle layer index (MLI) with the base layer moduli (E_2) for the measures taken in 2021

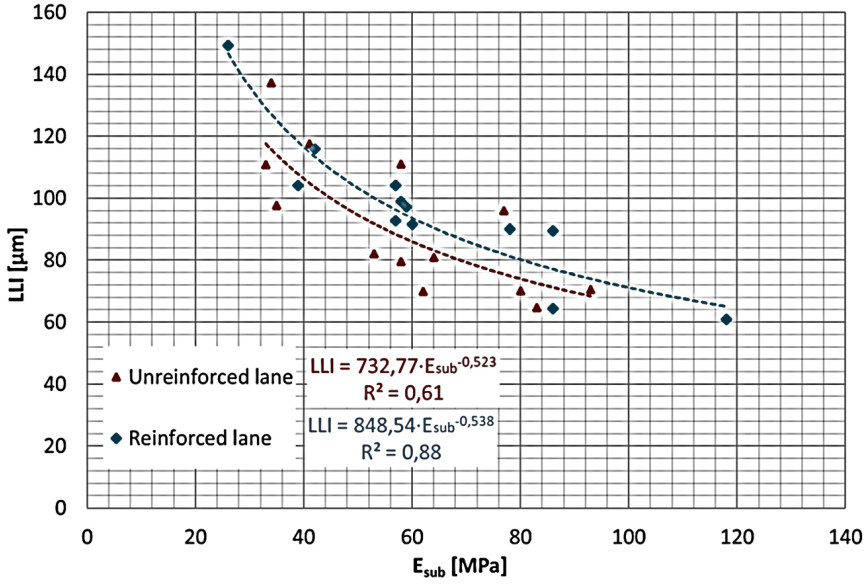

Fig. 10. A comparison of the lower layer index (LLI) with the subgrade moduli (E_{sub}) for the measures taken in 2021

4. Conclusions

The deflection basin parameters allowed the investigation of the technical condition of the different sections of the pavement: the upper layers consisted of asphalt concrete, the subbase layers consisted of crushed stone and the subgrade. Additional research shows that the applied reinforcement positively influences the technical state of the asphalt layers. It is reflected in higher values of the radius of curvature of the reinforcement lane. The rest of the deflection bowl parameters do not show such an impact, and the values differ between the lanes, usually indicating a poor technical condition of the pavement layers. The relationships observed between DBPs and backcalculated pavement layer moduli have shown the impact of applied reinforcement on the results. In this case, the correlations were observed in 2019 in every lane between moduli values and DBP-s; however, in 2021 the relationships for RoC, BLI, and MLI were observed only in the unreinforced lane. This may suggest that the degradation of the technical condition affected the results and the reinforced lane no longer produces reliable results. Additional analysis of the interlayer bonding on the obtained deflection measures could help to define why correlations were not observed in 2021 in the reinforced lane. However, this would indicate the influence of applied reinforcement on the obtained results more than on the technical condition of the pavement. The only observed relationship unaffected by reinforcement is LLI–E_{sub}, as it was observed in 2019 and 2021 and is strong for both the unreinforced and reinforced lane. In the moduli of case of the BLI and bituminous layers (E_1), it may be possible that the results may depend on the moduli of the crushed stone aggregate base due to relatively thick asphalt layers. The verification of the pavement layers thickness influence on determined correlations will also be carried out in further analysis together with the mechanistic empirical approach. The technical condition of the roads analysed may have influenced the data obtained. However, the differences between reinforced and unreinforced lanes were found. This is an interesting example of how the applied reinforcement affects the DBPs and their relationships with the back-calculated layer moduli. This is still an up-to-date topic among nondestructive methods to assess and evaluate the technical condition of the pavement. Since pavement may produce the same deflection value but completely different structural behaviours described by deflection basin shape, presented results and relationships are another step into developing an alternative approach to determining the initial pavement moduli i.e. to use as a seed moduli.

References

[1] J. Kawalec, M. Grygierek, E. Koda, and P. Osiński, "Lessons learned on geosynthetics applications in road structures in Silesia Mining Region in Poland", *Applied Sciences*, vol. 9, no. 6, pp. 1–14, 2019, doi: 10.3390/app9061122.

[2] M. Zięba, P. Kalisz, and M. Grygierek, "The impact of mining deformations on road pavements reinforced with geosynthetics", *Archives of Mining Sciences*, vol. 65, no. 4, pp. 751–767, 2020, doi: 10.24425/ams.2020.134145.

[3] E. Pietrzyk-Sokulska, R. Uberman, and J. Kulczycka, "The impact of mining on the environment in Poland – myths and reality", *Gospodarka Surowcami Mineralnymi – Mineral Resources Management*, vol. 31, no. 1, pp. 45–64, 2015, doi: 10.1515/gospo-2015-0009.

[4] K. Kłosek, J. Sobolewski, and J. Ajdukiewicz, "Protection systems of high tensile strength geosynthetics reinforcement together with electronic permanent monitoring used in several sections of A1 Motorway situated in heavy mining active terrain in Poland", *Transportation Overview*, no. 5-6, pp. 20–25, 2011 (in Polish).

[5] J. Kawalec, K. Chlipalski, and M. Grygierek, "Komunikacyjne obiekty liniowe na terenach górniczych. Roads in a mining subsidence area", *Magazyn Autostrady*, no. 3, pp. 35–42, 2015 (in Polish).

[6] J. Górszczyk and S. Gaca, "The influence of the carbo-glass geogrid-reinforcement on the fatigue life of the asphalt pavement structure", *Archives of Civil Engineering*,vol. 58, no. 1, pp. 97–113, 2012, doi: 10.2478/v.10169-012-0006-z.

[7] Z. Liu and H. Ling, "Performance of geosynthetic-reinforced asphalt pavements", *Journal of Geotechnical and Geoenviromental Engineering*, vol. 127, no. 2, pp. 177–184, 2001, doi: 10.1061/(ASCE)1090-0241(2001)127:2(177).

[8] P. Jaskuła, D. Ryś, M. Stienss, C. Szydłowski, M. Gołos, and J. Kawalec, "Fatigue performance of double-layered asphalt concrete beams reinforced with new type of geocomposites", *Materials*, vol. 14, no. 9, 2021, doi: 10.3390/ma14092190.

[9] L. Nguyen, J. Blanc, J. Kerzerho, and P. Hornych, "Review of glass fibre grid use for pavement reinforcement and APT experiments at IFSTTAR", *Road Materials and Pavements Design*, vol. 14, pp. 287–308, 2013, doi: 10.1080/14680629.2013.774763.

[10] I. Arsenie, C. Chazallon, J. Duchez, and P. Hornych, "Laboratory characterisation of the fatigue behaviour of glass-fibre grid-reinforced asphalt concrete using 4PB tests", *Road Materials and Pavement Design*, vol. 18, no. 1, pp. 168–180, 2017, doi: 10.1080/14680629.2016.1163280.

[11] L. Jong-Hoon, B. Seung-Beom, L. Kang-Hoon, K. Jo-Soon, and J. Jin-Hoon, "Long-term performance of fibre-grid-reinforced asphalt overlay pavements. A case study of Korean national highways", *Journal of Traffic and Transportation Engineering*, vol. 6, no. 4, pp. 366–382, 2019, doi: 10.1016/j.jtte.2018.01.008.

[12] S. Baltzer and G. Hilderbrand, *HSD Measurements at the BAST Test Track - COST 354: Short Term Scientific Mission*, 2006. Danish Road Directorate, 2007.

[13] J. Eijbersen and J. Van Zwieten, "Application of FWD measurements at the network level", in *4th International Conference on Managing Pavements: 17–21 May 1998: International Convention Centre (ICC), Durban, South Africa*, vol. 1. Pretoria, South Africa, 1988, pp. 438–450.

[14] A. Pożarycki, P. Górnaś, M. Bilski, and A. Turkot, "Parametrisation of deflection curve flexible pavement", *Drogownictwo*, no. 3, pp. 67–73, 2019 (in Polish).

[15] S. Węgliński, M. Flieger-Szymańska, M. Just, and D. Krawczyk, "Ground improvement and rebuild of a district roadin complex geotechnical-engineering conditions – case study", *Archives of Civil Engineering*, vol. 68, no. 2, pp. 63–82, 2022, doi: 10.24425/ace.2022.140630.

[16] O. Talvik and A. Aavik, "Use of FWD deflection basin parameters (SCI, BDI, BCI) for pavement condition assessment", *The Baltic Journal of Road and Bridge Engineering*, vol. 4, no. 4, pp. 196–202, 2009, doi: 10.3846/1822-427X.2009.4.196-202.

[17] M. Rocha, G. Marques, and R. Silva, "Predicting equations for determining layer elastic moduli by using Deflection Basin Parameters (DBPs) from Falling Weight Deflectometer", *International Journal of Pavement Engineering*, vol. 23, no. 13, pp. 4708–4720, 2022, doi: 10.1080/10298436.2021.1972296.

[18] M. Rocha, G. Marques, R. Silva, and G. Lana, "Influence of seed layer moduli on backcalculation procedure and on overlay design of flexible pavements", *Transportation Research Record*, vol. 2676, no. 5, pp. 341–357, 2022, doi: 10.1177/03611981211065753.

Zależności pomiędzy wskaźnikami czaszy ugięć a modułami warstw uzyskanymi z obliczeń odwrotnych

Słowa kluczowe: czasza ugięć, obliczenia odwrotne, siatka z włókna szklanego, ugięciomierz FWD, wskaźniki krzywizny

Streszczenie:

Przedmiotem niniejszego opracowania jest droga powiatowa na której, podczas prac remontowych, zastosowano wzmocnienie siatką z włókna szklanego. Wzmocniono jeden pas ruchu natomiast drugi pozostawiono bez wzmocnienia. Odcinek testowy posłużył do badania oraz analizy wpływu wzmocnienia na zależności pomiędzy wartościami wybranych wskaźników krzywizny czaszy ugięć a modułami uzyskanymi z obliczeń odwrotnych. Przeprowadzono badania ugięciomierzem FWD, następnie wyznaczono wybrane wskaźniki krzywizny czaszy ugięć oraz moduły warstw konstrukcji jezdni. Wyniki zestawiono dla pomiaru z 2019 roku oraz kontrolnego z 2021 roku. Zaobserwowano zależności pomiędzy obliczonymi wskaźnikami czaszy ugięć a modułami warstw nawierzchni uzyskanymi z obliczeń odwrotnych. Pas wzmocniony wykazywał wyższe wartości współczynnika determinacji pomiędzy wartościami wskaźników krzywizny czaszy ugięć a wartościami modułów warstw nawierzchni w roku 2019 lecz pomiar w roku 2021 nie potwierdził ich występowania, poza LLI. Na pasie niewzmocnionym zaobserwowano dobrą zgodność funkcji opisującej analizowane zależności zarówno w roku 2019, jak i 2021. Z uwagi na stosunkowo małą liczbę punktów pomiarowych oraz na specyfikę porównywanych danych prowadzone obserwacje należy traktować jako wstępne.

Received: 2023-05-08, Revised: 2023-06-23